Computers in Industry 139 (2022) 103645

Contents lists available at ScienceDirect

Computers in Industry

journal homepage: www.elsevier.com/locate/compind

A hierarchical Bayesian regression framework for enabling online reliability estimation and condition-based maintenance through accelerated testing

Leonardo Leoni[a], Filippo De Carlo[a,*], Mohammad Mahdi Abaei[b], Ahmad BahooToroody[c]

[a] Department of Industrial Engineering (DIEF), University of Florence, Italy
[b] Department of Maritime and Transport Technology, Delft University of Technology, Delft, The Netherlands
[c] Marine and Arctic Technology Group, Department of Mechanical Engineering, Aalto University, Finland

A R T I C L E I N F O

Article history:
Received 19 October 2021
Received in revised form 7 March 2022
Accepted 8 March 2022
Available online 21 March 2022

Keywords:
Condition monitoring
Condition-based maintenance
Hierarchical Bayesian regression
Generalized linear model
Online reliability estimation

A B S T R A C T

Thanks to the advances in the Internet of Things (IoT), Condition-based Maintenance (CBM) has progressively become one of the most renowned strategies to mitigate the risk arising from failures. Within any CBM framework, non-linear correlation among data and variability of condition monitoring data sources are among the main reasons that lead to a complex estimation of Reliability Indicators (RIs). Indeed, most classic approaches fail to fully consider these aspects. This work presents a novel methodology that employs Accelerated Life Testing (ALT) as multiple sources of data to define the impact of relevant PVs on RIs, and subsequently, plan maintenance actions through an online reliability estimation. For this purpose, a Generalized Linear Model (GLM) is exploited to model the relationship between PVs and an RI, while a Hierarchical Bayesian Regression (HBR) is implemented to estimate the parameters of the GLM. The HBR can deal with the aforementioned uncertainties, allowing to get a better explanation of the correlation of PVs. We considered a numerical example that exploits five distinct operating conditions for ALT as a case study. The developed methodology provides asset managers a solid tool to estimate online reliability and plan maintenance actions as soon as a given condition is reached.

1. Introduction

In recent years, the advances related to the Internet of Things (IoT) technology have facilitated the implementation of an effective Condition-Based Maintenance (CBM) policy (Morimoto et al., 2017) (previously known as predictive maintenance policy (Prajapati et al., 2012)). The development of newer sensors and advanced data mining and feature extraction techniques have led to a more accurate condition monitoring process. The major advantage of CBM compared to other Preventive Maintenance (PM) policies is the ability to schedule maintenance actions depending on the monitored condition of an asset, rather than planning maintenance interventions based on reliability parameters such as the Mean Time To Failure (MTTF). Although CBM requires more efforts related to the installment of sensors and much more responsiveness compared to Time-Based or Aged-Based PM regarding logistics aspects and maintenance squad deployment, it could lead to a lower waste of equipment useful life. According to the aforementioned statements, CBM has attracted the attention of many researchers over the past decade (Cipollini et al., 2018; Hao et al., 2020; Hu et al., 2021; Jiang et al., 2021; Omshi and Grall, 2021; Xu et al., 2021).

We could divide any CBM policy into three consecutive steps, which are denoted as (i) data acquisition, (ii) data processing, and (iii) maintenance decision-making (Jardine et al., 2006). The first step consists of collecting useful data, usually from sensors, while during the second one, noise components are filtered out from the physical observations, and subsequently, data analysis is conducted. The combination of data acquisition and data processing is regarded as condition monitoring, representing a precursor of any CBM. Finally, it is worth mentioning that distinct kinds of condition monitoring could be implemented, such as online condition monitoring (Wang et al., 2020), quasi-online condition monitoring (Zhang et al., 2021), and remote condition monitoring (Memala et al., 2021).

Within the process of condition monitoring, there is a distinction between classification and regression approaches. A classification approach aims at identifying the state of an asset-based on the monitored parameters. On the other hand, a regression framework

* Corresponding author.
E-mail address: filippo.decarlo@unifi.it (F. De Carlo).

https://doi.org/10.1016/j.compind.2022.103645
0166-3615/

aims to evaluate how a given response variable denoting the degradation of the system develops in time based on some monitored parameters. Moreover, in classification problems, the response variable is categorical, while in regression methods, the response variable is real-valued (Murphy, 2012). Since condition monitoring plays a pivotal role in conducting an efficient and effective CBM plan, there is an ongoing effort for both classifications (Brito et al., 2022; Potočnik and Govekar, 2017; van den Hoogen et al., 2021) and regression purposes (Dave et al., 2021; Ferrando Chacón et al., 2021). This fundamental vision has resulted in the adoption of a wide variety of tools such as autoregressive moving average (ARMA) (Baptista et al., 2018), Fast Fourier Transform (FFT) (Gowid et al., 2015), FFT combined with SVM (Pandarakone et al., 2017) and wavelet approach (Benkedjouh et al., 2018). The aforementioned tools can analyze an input signal, eventually, remove noisy components, and study the degradation of devices. A relevant example is a work proposed by Gowid et al. (2015), who applied FFT to analyze acoustic data and perform fault diagnosis in a centrifugal device. FFT is also used for fault detection of bearings by Pandarakone et al. (2017), who subsequently adopted SVM for fault diagnosis. All the aforementioned methods present some limitations. For instance, ARMA is characterized by a tuning process to determine the most accurate parameters of the model, while FFT could lead to a loss of features that vary over time because of its integral nature.

Meanwhile, Bayesian inference, such as Bayesian Network (BN) and Hierarchical Bayesian Modelling (HBM), has also become a popular tool for condition monitoring purposes, thanks to its features, among which the ability to deal with source-to-source variability (Kumari et al., 2020). Moreover, Bayesian Inference can provide better results than other parametric regression methods, such as Maximum Likelihood Estimation (MLE) (BahooToroody et al., 2020a). Finally, the adoption of a hierarchy structure allows addressing the correlations among nonlinear data and the variation of non-stationary data, leading to a more coherent regression model compared to other classic approaches (BahooToroody et al., 2019b). A relevant example of a BN-based condition monitoring approach is presented by BahooToroody et al. (2019b). In their paper, they integrate an Empirical Mode Decomposition with a Statistical Significant Test for noise removal, while they employ a Bayesian Network with a hierarchical structure to predict the time of the following pressure exceedance. Another recent work by BahooToroody et al. (2020b) presented an HBR model to determine the probability of failure of a natural gas regulating and metering station based on the monitored pressure. In their work, they modeled a discrete response variable through a normal logit GLM, considering the pressure as the independent variable. Bayesian Inference has been proven itself as a solid tool for reasoning under uncertainty, however, it presents some drawbacks. Specifically, Bayesian Inference is characterized by a greater mathematical complexity compared to other classical approaches. The mathematical complexity requires a higher degree of knowledge and it could lead to greater calculation time. However, the advances of specific tools have reduced the calculation time and have taken easier the implementation of the Bayesian analysis. Moreover, the choice of the prior distribution could be tough and an improper choice could lead to some undesired results. To avoid issues related to the calculation time, a non-informative prior could be used.

1.1. Background on accelerated life testing

Within the context of reliability estimation, one of the main issues is related to data scarcity. Indeed, most probabilistic and reliability analysis suffers from a lack of data (Z. S. Ye and Xie, 2015), leading to high uncertainty in the estimation procedures (El-Gheriani et al., 2017). To overcome such limitations and satisfy reliability requirements, Accelerated Life Testing (ALT) has become a common practice over the past few years (Escobar and Meeker, 2006). In ALT, a given component is tested under operating conditions that are more severe than the standard operating condition (e.g., higher pressure than the nominal working pressure) (Elsayed, 2012), leading to a premature failure. Accordingly, ALT allows to observe and to collect failure data in a shorter amount of time compared to real-world application, resulting in safer operations. Moreover, making ALT before producing or selling a piece of equipment gives more flexibility and precision during the definition of maintenance or insurance policies.

ALT is treated through one of the following models (Moustafa et al., 2021): (I) statistical models, (II) frailty models and (III) distribution-free models. The first category of models assumes that the failure times follow a given distribution with one or more parameters that depend upon the operating condition. The statistical models are fully parametric and they allow to fit to the data different kinds of distributions such as Weibull (Lin et al., 2017) or exponential (Haghighi, 2014). On the other side, the second group of models exploits a random factor called frailty, which influences the hazard function of the latent lifetimes (Liu, 2012). Examples of frailty model adoption can be found in Z.-S. Ye et al. (2013) and Roy (2018). Finally, the distribution-free models fall within the nonparametric approaches and they have the advantage to avoid the requirement of finding a distribution that can properly fit the available data. Even though non-parametric models could lead to conservative results and do not require any distribution specification, parametric approaches such as statistical models could generate more accurate results given a proper choice of the distribution (Thomas, 2015). Furthermore, they conceal more physical meaning, leading to a more informative description of the problem.

Within the context of ALT, degradation data could be exploited instead of lifetime data during ALT. In this case, the evolution of one or more degradation parameters is studied and a degradation model is fit over the data. Degradation data contain more information compared to lifetime data, however, great knowledge of the equipment is required to choose a proper degradation parameter. Furthermore, linking the degradation to a RI should be based on sound reliability requirements (Thomas, 2015). It follows that building a degradation model could not always be a viable option. Considering the aforementioned statements, a lifetime parametric model is chosen for this study.

To conclude this section, it is worthwhile mentioning that Bayesian Inference has progressively become more popular to deal with ALT. A recent work by Moustafa et al. (2021) integrates frailty models and Bayesian inference to estimate the reliability of a multicomponent system through ALT conducted both at the component and system level. Particularly, in their work, the authors employed the shared frailty model to address the relationships among the failures of distinct components, while the Bayesian framework is adopted to incorporate the information coming from the component and the system level. Another recent work by Pang et al. (2021) exploited an HBM and ALT to predict the RUL of a jewel-bearing accelerometer. First, ALT is conducted to determine the distribution type and estimate the hyper-parameters of an HBM, which is later exploited to update the posterior distribution based on condition monitoring data. In the present work, ALT is exploited to extrapolate a relation between PVs and RIs through HBR, rather than finding an informative prior for Bayesian inference.

1.2. Research gap and aim

Despite all ongoing efforts, little attention has been devoted to determining how fluctuations in PVs influence RIs (BahooToroody et al., 2019a), which is essential to grasp the changes in risk over time. Moreover, most of the approaches related to condition monitoring of RIs fail to consider nonlinear correlation and multiple sources of data. As a result, developing a robust parametric tool capable of estimating an asset's reliability performance over time, based on monitored operational parameters and subsequently plan maintenance actions, is welcome. To this end, a methodology able to schedule maintenance according to the variation of PVs is presented in this paper. For this purpose, after extracting failure data from ALT, an HBR is employed to estimate the characteristic parameters of a GLM linking the PVs and one RI. Lifetime data are considered instead of degradation data due to the less knowledge requirement and the easiness to link a RI. In this context, the most common approach, which is the MLE (Pascual et al., 2006), neglects the variability among distinct sources of data. Conversely, a Bayesian network with a hierarchical structure allows us to consider source-to-source variability, leading to an accurate explanation of the correlation of PVs even when multiple data sources are present. Moreover, Bayesian approaches allow users to insert available knowledge, which could be considered as supplementary data. This feature could also be useful to drive the analysis in case of data scarcity when expert judgments or prior knowledge are available. For instance, within the context of ALT, the distribution coming from similar equipment could be used as a prior choice, reducing the number of tests to perform. However, the amount of information inserted within the prior distribution should be dosed carefully to avoid a completely prior driven calculation. On the other hand, the adoption of GLM allows overcoming the main limitation of the parametric statistical-based models, which is fitting a specific distribution to the data. Indeed, GLMs are more flexible compared to other approaches since they can consider a wide range of probability distributions for the data, bypassing the assumption of normal error relationships between independent and dependent variables (Guisan et al., 2002). Furthermore, they have demonstrated high efficiency and the ability to deal with nonnormal response variables (Yeganeh and Shadman, 2021).

It is worthwhile mentioning that, in the context of reliability analysis, condition monitoring, and ALT, Bayesian techniques have become popular tools. However, few works related to HBM, and more specifically HBR, employed to process data coming from ALT are present. Besides, there is still space to consider a continuous response variable within an HBR framework as recommended by BahooToroody et al. (2020b). Finally, most of the statistical-based works related to ALT are mainly focused on determining the reliability parameters, while the subsequent exploitation of the statistical model from a condition monitoring perspective is disregarded. In contrast, this task is often carried out in case a degradation model has been implemented. Accordingly, during the last phase of the developed methodology, a proposal of maintenance tasks planning based on the monitored PVs and the subsequent online reliability estimation is presented. The developed framework is implemented on data extracted from ALT conducted with five distinct operating conditions.

The remainder of this paper is organized as follows; Section 2 describes the material and methods, while Section 3 is about the developed methodology. Section 4 illustrates the implementation of the methodologies in the numerical example adopted as a case study, while Section 5 discusses the results. Finally, conclusions and future developments are presented in Section 6.

2. Material and methods

2.1. Hierarchical Bayesian modeling

The main aim of any statistical inference is to deduce the properties or features of a population after analysing a sample of data extracted from the population itself. The HBM is a renowned statistical tool that allows conducting inference based on real-world observations through the Bayes Theorem (Eq. (1)) (El-Gheriani et al., 2017).

$$\pi_1(\theta|x) = \frac{f(x \mid \theta)\pi_0(\theta)}{\int_\theta f(x \mid \theta)\pi_0(\theta)d\theta} \tag{1}$$

where θ is often a vector that denotes the unknown parameters to infer. $\pi_1(\theta|x)$ identifies the posterior distribution, representing the updated knowledge on the parameters of interest after observing the available data and conducting the inference. The posterior distribution is given by the product of the likelihood function and the prior distribution, which are respectively referred to as $f(x|\theta)$ and $\pi_0(\theta)$. Accordingly, the Bayesian inference assigns a prior probability distribution to θ, rather than considering it as a fixed value such as the frequentist approaches (Garthwaite et al., 2002). Particularly, the HBM is named after exploiting a multistage or hierarchical prior, expressed by Eq. (2) (Kelly and Smith, 2011).

$$\pi_0(\theta) = \int_\varnothing \pi_1(\theta|\varphi)\pi_2(\varphi)d\varphi \tag{2}$$

where $\pi_1(\theta|\varphi)$ is called first-stage prior distribution, representing the variability of θ, while φ is a vector in case the distribution of θ is a multi-parameters distribution. For instance, let θ be characterized by a normal distribution, φ would be a two-element vector representing the mean and the standard deviation of the normal distribution. However, when θ is distributed as a single parameter distribution (e.g., exponential), φ would be a scalar number. The components of φ, which are called hyper-parameters, are distributed accordingly to the hyper-prior distribution denoted by $\pi_2(\varphi)$.

2.2. Generalized linear model

The GLMs represent a practical and more flexible extension of linear models. Indeed, a GLM allows a response variable to be correlated with the covariates through a given link function, as shown by Eq. (3) (Follmann and Wu, 1995).

$$g(Y) = \alpha_0 + \sum_{i=1}^{n}\sum_{j=1}^{m}\sum_{k=1}^{r}\alpha_i X_j^k \tag{3}$$

where $g(Y)$ represents the link function, while X_j are called covariates or predictors, or explanatory variables. Furthermore, α_0 identifies the intercept, α_i denotes the coefficients, k is an exponent integer, while n and m are the number of coefficients and predictors, respectively. Finally, Y is the response variable, which follows an exponential family distribution (e.g., normal, Poisson, or binomial) in a GLM.

For condition monitoring purposes, it is worthwhile mentioning that the response variable is a RI, e.g., the hazard rate or the meantime to failure, while the covariates are the monitored process variables, e.g., pressure or temperature. Thus, the link function defines the relationship between the RI (dependent variable) and the monitored process variables (independent variables).

2.3. Hierarchical Bayesian regression

This paragraph summarizes the procedure to perform HBR. The hyper-parameters of an HBR model are the intercept and the coefficients characterizing the link function. The prior distribution and the likelihood function are expressed through Eqs. (4) and (5), respectively [46].

$$\pi_0(\theta) = \int_{-\infty}^{+\infty}\int_{-\infty}^{+\infty}\ldots\int_{-\infty}^{+\infty}\pi_1(\theta|\alpha_0, \alpha_1\ldots\alpha_n)\pi_2(\alpha_0, \alpha_1\ldots\alpha_n)\partial\alpha_0\partial\alpha_1\ldots\partial\alpha_n \tag{4}$$

$$f(Y|\alpha_0, \alpha_1\ldots\alpha_n) = \int_\Theta f(Y|\theta)\pi_1(\theta|\alpha_0, \alpha_1\ldots\alpha_n)d\theta \tag{5}$$

where $\pi_1(\theta|\alpha_0, \alpha_1\ldots\alpha_n)$ and $\pi_2(\alpha_0, \alpha_1\ldots\alpha_n)$ are the first-stage prior and the hyper-prior, respectively. Through Bayes' Theorem (Eq. (1)), the posterior distribution of the hyper-parameters is got by Eq. (6) (Zeger and Karim, 1991).

$$\pi_1(\alpha_0, \alpha_1 ... \alpha_n|Y) = \frac{[\int_\Theta f(Y|\theta)\pi_1(\theta|\alpha_0, \alpha_1...\alpha_n)d\theta]^*[\int_{-\infty}^{+\infty}\int_{-\infty}^{+\infty}...\int_{-\infty}^{+\infty}\pi_1(\theta|\alpha_0, \alpha_1...\alpha_n)\pi_2(\alpha_0, \alpha_1...\alpha_n)\partial\alpha_0\partial\alpha_1...\partial\alpha_n]}{\int_\Theta[\int_\Theta f(Y|\theta)\pi_1(\theta|\alpha_0, \alpha_1...\alpha_n)d\theta]^*[\int_{-\infty}^{+\infty}\int_{-\infty}^{+\infty}...\int_{-\infty}^{+\infty}\pi_1(\theta|\alpha_0, \alpha_1...\alpha_n)\pi_2(\alpha_0, \alpha_1...\alpha_n)\partial\alpha_0\partial\alpha_1...\partial\alpha_n]d\theta} \tag{6}$$

In a Markov Chain Monte Carlo (MCMC) process, the posterior distribution is often estimated numerically by Gibbs sampling by exploiting the conjugate prior. Given a certain likelihood, choosing a conjugate prior makes the form of the posterior known. It is also possible to adopt a non-conjugate prior distribution, but it will lead to higher mathematical complexity. Moreover, the property of the conjugate prior allows the Gibbs algorithm to find the posterior distribution by first randomly sampling from both the prior distribution (Eq. (4)) and the likelihood function (Eq. (5)), and subsequently applying the Bayes' Theorem. Finally, the posterior predictive distribution for the unknown parameter of interest (θ) is given by Eq. (7).

$$\pi(\theta|Y) = \int_{-\infty}^{+\infty}\int_{-\infty}^{+\infty}...\int_{-\infty}^{+\infty}\pi_1(\theta|\alpha_0, \alpha_1...\alpha_n)\pi_1(\alpha_0, \alpha_1...\alpha_n|Y)\partial\alpha_0\partial\alpha_1...\partial\alpha_n \tag{7}$$

Accordingly, the posterior predictive distribution shown in Eq. (7) is obtained by MCMC via a sampling process of the joint posterior distributions of the hyper-parameters.

The remainder of this paper is organized as follows; Section 2 describes the methodology developed. Section 3 illustrates the implementation of the methodologies in the numerical example adopted as a case study, while Section 4 discusses the results. Finally, conclusions are presented in Section 5.

3. Developed methodology

Identifying a relationship between PVs and RIs represents a pivotal task in grasping the changing of reliability factors during operation. To this end, the primary goal of this paper is to develop a methodology that can correlate RIs and PVs (1) and estimate online reliability to schedule maintenance tasks (2). The sequence of the proposed four-stage framework is presented in Fig. 1.

3.1. Stage 1: experimental tests and data collection

In the proposed method, ALT with fixed PVs are performed on a given device (Step 1), and subsequently, Times To Failure (TTFs) are extracted (Step 2). Each ALT identifies a source of data that is later exploited to build the regression model.

3.2. Stage 2: hierarchical Bayesian regression

We chose different GLMs to test them on the acquired failure data (Step 3). Indeed, testing more than one model can be practical since the relationship between the reliability indicator and the PVs is not clear, and more than one valid relationship can exist. In the

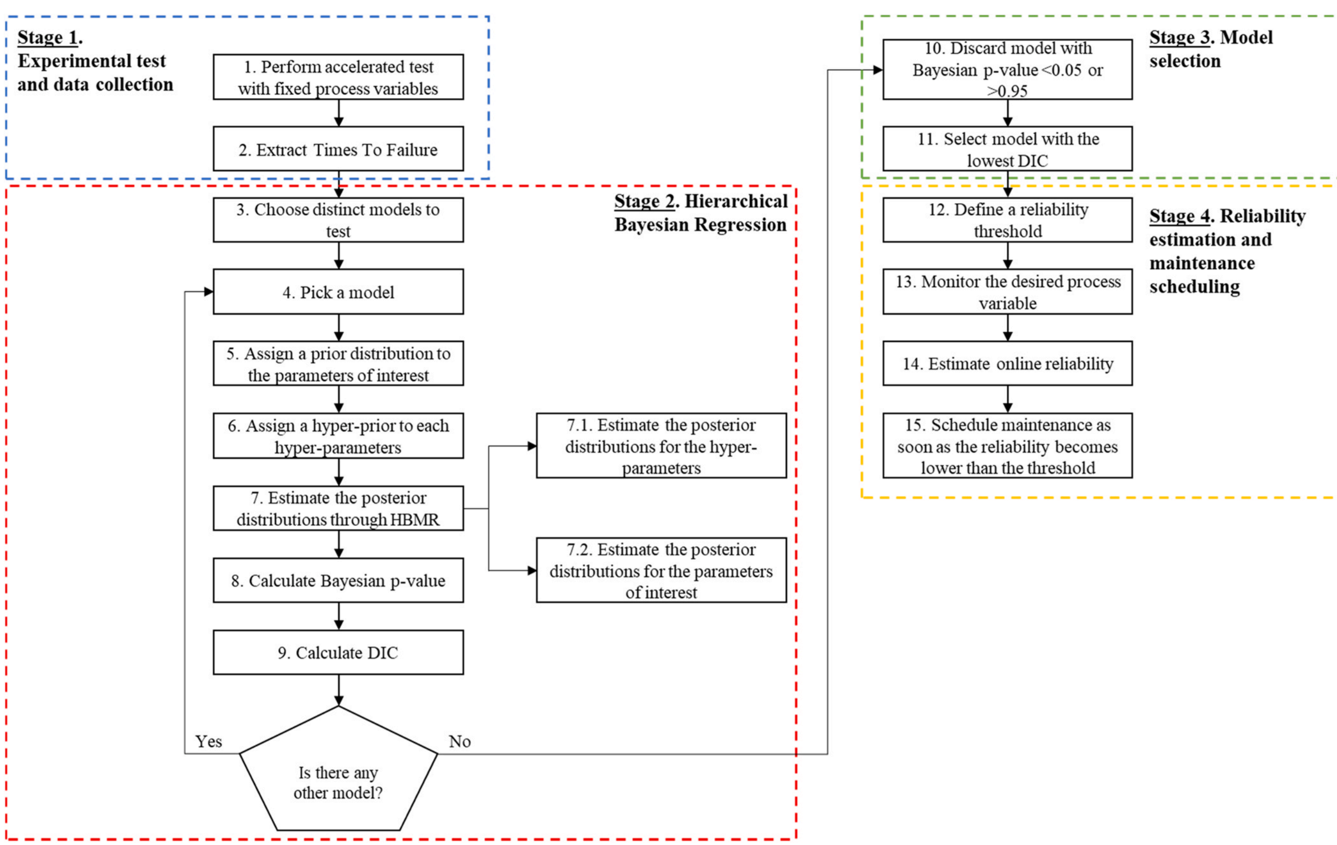

Fig. 1. Developed framework for online reliability estimation with HBR and GLM.

second case, the relationship that allows modeling the data properly and simultaneously allows minimizing the complexity of the model must be chosen. The choice of the models should be based on expert judgment, available physical knowledge of the deterioration process, or historical data (BahooToroody et al., 2020b). After choosing the models, they are tested separately and independently (Step 4). At first, prior distributions are assigned to both the parameters of interest (Step 5) and the hyper-parameters (Step 6). The choice of the prior distribution could be based on knowledge or could be non-informative. In the latter case, the inference will be completely data-driven, since a non-informative prior is very diffusive and spread over the variables' domains (e.g., a uniform prior). Besides, it is worthwhile mentioning that choosing a conjugate prior is usually convenient for mathematical purposes since it allows to obtain a closed-mathematical solution. After setting the prior distributions, the HBR is performed to get the posterior distribution of the hyperparameters and the parameters of interest (Steps 7.1–7.2). Finally, the Bayesian p-value and the Deviance Information Criterion (DIC) are estimated (Steps 8–9). The Bayesian p-value determines the goodness of fit, while the DIC, given by Eq. (8), is exploited to compare distinct models.

$$DIC(\theta) = -2\log(f(Y|\theta)) \tag{8}$$

where $f(Y|\theta)$ is the likelihood function. The DIC is composed of two penalized functions: the first one considers the goodness of fit, while the second function evaluates the complexity of the model. Thus, assuming equal goodness of fit, the higher the complexity of the model, the higher the DIC.

3.3. Stage 3: model selection

Since more models are tested on the available data, a criterion to pick one model over the others must be chosen. The p-value compares the observations with the predicted values obtained through the posterior distribution. In other words, the p-value determines how well the model replicates the data. Particularly, a p-value lower than 0.05 denotes a model that generates much higher values than the observed data, while a p-value higher than 0.95 is associated with a model which predicts much lower values compared to the observations. Consequently, the mean p-value should be around 0.5 (Kelly and Smith, 2011), and in this study, every model whose mean p-value is less than 0.05 or higher than 0.95 is discarded (Step 10). Next, the remaining models are compared through the DIC; specifically, the model with the lowest DIC is selected (Step 11).

3.4. Stage 4: reliability estimation and maintenance scheduling

Assuming that the considered device is working in standard operation, the fourth stage of the methodology is implemented. First, a reliability threshold is defined (Step 12). Indeed, critical equipment maintenance is usually scheduled as soon as a given reliability threshold is reached, rather than considering fixed indicators such as the Mean Time To Failure (MTTF). Subsequently, the PVs characterizing the selected GLM are monitored (Step 13), and the reliability of the component is computed at each time unit (Step 14). At last, maintenance is planned when the estimated reliability becomes lower than the aforementioned threshold (Step 15).

4. Results: application of the methodology

To show the applicability of the method, we used a numerical example as a case study.

4.1. Stage 1: experimental tests and data collection

We considered pressure and temperature as process variables for the ALT. Five distinct Operating Conditions (OC) with five levels of pressure and two levels of temperature are evaluated. For each operating condition, ten components are tested until failure (step 1), and the TTFs are extracted (step 2). This kind of ALT is usually called run-to-failure because the test is carried on until a failure occurs. However, the ALT may manage censored data since the tests are conducted for a limited period. Even if censored TTFs are not considered for this numerical example, they could easily be included in the analysis. It is also worthwhile mentioning that the number of operating conditions and components to test should be chosen based on company policies, available knowledge, and expert judgment. Considering as an example the study presented by Tucci et al. (2014), twenty-four components are tested in three distinct OCs, while in the work of Hamada et al. (2008) an example of forty components and four OCs is reported. Given the aforementioned examples, the authors considered fifty components in five distinct OCs. The analysed OCs and the extracted TTFs are listed in Tables 1 and 2, respectively.

4.2. Stage 2: hierarchical Bayesian regression

The third step of the methodology requires the specification of distinct models to test the data. The TTF distribution should be chosen based on prior beliefs and knowledge of the failure process. In this study, we assumed the TTF to follow a normal distribution, thus normal-normal regression models are considered:

$$TTF \sim N(\mu, \sigma^2) \tag{9}$$

Accordingly, the parameters of interest are the MTTF (μ) and the standard deviation (σ). Furthermore, the canonical link function for the normal-normal regression model is the identity function, as shown by Eq. (10).

$$\mu = MTTF = \alpha_0 + \sum_{i=1}^{n}\sum_{j=1}^{m}\sum_{k=1}^{r}\alpha_i X_j^k \tag{10}$$

Based on the previous paragraph, the Bayesian regression aims to determine the relationship between the MTTF and the PVs (i.e., pressure and temperature); therefore, two distinct models are developed, as shown in Eqs. (11) and (12), respectively.

$$\mu = MTTF = a + b^*Press + c^*Temp \tag{11}$$

$$\mu = MTTF = a + b^*Press \tag{12}$$

Table 1
Considered OCs for the accelerated testing procedure.

PV	OC1	OC2	OC3	OC4	OC5
Pressure [bar]	8	9	10	11	12
Temperature [°C]	30	30	30	40	40

Table 2
TTFs (hours) extracted from the accelerated tests for each OC.

TTF	OC1	OC2	OC3	OC4	OC5
TTF1	113.61	107.20	95.91	71.21	67.65
TTF2	92.35	82.60	83.21	74.47	66.66
TTF3	104.15	93.18	93.31	94.89	43.98
TTF4	101.07	98.53	84.75	63.64	72.23
TTF5	112.17	102.64	89.14	68.73	75.53
TTF6	91.64	103.43	90.49	69.53	73.09
TTF7	118.12	94.57	87.37	81.56	67.07
TTF8	94.69	108.52	68.09	74.12	69.15
TTF9	99.41	83.72	56.95	63.54	71.44
TTF10	104.16	83.74	91.72	79.16	61.04

where a denotes the intercept, while b and c are the pressure and temperature coefficients, respectively. In the first model, the influence of both pressure and temperature on MTTF is investigated, while the second model addresses how pressure variations affect the MTTF. To conclude, the assignment of a prior distribution to each parameter of interest (step 5), a non-informative gamma prior is chosen for the standard deviation (Eq. (13)). Indeed, the gamma prior is the natural conjugate prior for the standard deviation, allowing for obtaining a closed-mathematical solution. Moreover, choosing a non-informative prior allows comparing the results of HBM and other estimation approaches such as MLE (D. L. Kelly and Smith, 2009).

$$\sigma \sim Gamma(0.0001\ ,\ 0.0001) \tag{13}$$

Next, the prior distributions for the hyper-parameters are defined (step 6). In the first model, there are three hyper-parameters (the intercept a, and the slopes b and c), while in the second model, there are two hyper-parameters (the intercept a and the slope b). Adopting non-informative priors is strongly recommended when enough data is available to avoid a powerful influence (of the prior choice) on the posterior distribution (Leoni et al., 2021). For each hyper-parameter, a diffusive normal prior is selected:

$$a \sim N(0\ ,\ 10^4) \tag{14}$$

$$b \sim N(0\ ,\ 10^4) \tag{15}$$

$$c \sim N(0\ ,\ 10^4) \tag{16}$$

The next phase is the development of the Bayesian regression, which is implemented through RJags. To predict the posterior distributions (step 7), the MCMC sampling process is conducted with three chains characterized by over-dispersed initial values. Considering over one chain is strongly recommended to check the convergence of the process. Each chain is simulated with 10^5 iterations preceded by 1000 burn-in iterations. The statistical summaries of the posterior distributions of the hyper-parameters are reported in Tables 3 and 4 for the first and second models, respectively. Fig. 2 illustrates the MCMC chains of the first model, while Fig. 3 shows the MCMC chains related to the second model.

Each color of Figs. 2 and 3 denotes a different chain. The convergence of the second model is successful since the three chains are well-mixed as depicted by the left graph of Fig. 3. For the first model (Fig. 2), the trace plots of the pressure (b) and the temperature (c) coefficient show a worse convergence compared to the second model. However, for both models, the Gelman indexes related to the predicted parameters are equal to 1 or very close to 1. The Gelman index estimates the ratio of the within-chain variance and the between-chain variance. Thus, a Gelman index close to 1 indicates that the variance within-chain and between-chain are similar, which is an indicator of convergence. Furthermore, as revealed in Table 3, the influence of the temperature is much lower compared to the relevance of the pressure. Indeed, the temperature coefficient is lower than the pressure coefficient in the first model. The aforementioned considerations could be useful to make an informed decision on the model to pick, however, the following steps are required for a more in-depth and conscientious choice. Indeed, there are some scenarios characterized by equally suitable models when trace-plots, Gelman index, and estimated parameters are the only considered factors. The validity of the developed models is determined by estimating the Bayesian p-value (Step 8), while the choice of the model is guided by the DIC (Step 9). For the first model, the mean p-value was equal to 0.4977, while the calculation revealed a mean p-value of 0.5004 for the second model. The first model is characterized by a DIC equal to 374.6, while a DIC of 374.2 is associated with the second regression model.

4.3. Stage 3: model selection

The validity of both regression models is proved through the Bayesian p-value, which is close to 0.5, thus no model is discarded (Step 10). Furthermore, the DIC of the second model is slightly lower than the DIC associated with the first model. Accordingly, the second model is selected, and it is considered for the remaining part of this paper (Step 11).

To further prove the goodness of the model, the cost function illustrated by Eq. (17) is adopted.

$$Cost\ function = \frac{1}{2n}\sum_{i=1}^{n}(Pred_i - Obs_i)^2 \tag{17}$$

where n denotes the number of observations, while $Pred_i$ and Obs_i are the ith prediction of the model and the ith observed value, respectively. The cost function is calculated for each value of the intercept (a) and the slope (b) within their respective 95% credible interval (listed in Table 4), using a discretization of 0.1. The cost

Table 3
Statistical summary of the posterior parameters of the first model.

Parameter	Mean	Standard Deviation	2.5 percentile	97.5 percentile
a	178.023	10.3954	157.909	198.534
b	-9.0718	1.9926	-13.027	-5.234
c	-0.0752	0.5714	-1.147	1.072
sigma	10.0079	1.0569	8.193	12.326

Table 4
Statistical summary of the posterior parameters of the second model.

Parameter	Mean	Standard Deviation	2.5 percentile	97.5 percentile
a	177.391	9.964	157.62	196.707
b	-9.2645	0.9866	-11.172	-7.307
sigma	9.9118	1.0352	8.135	12.188

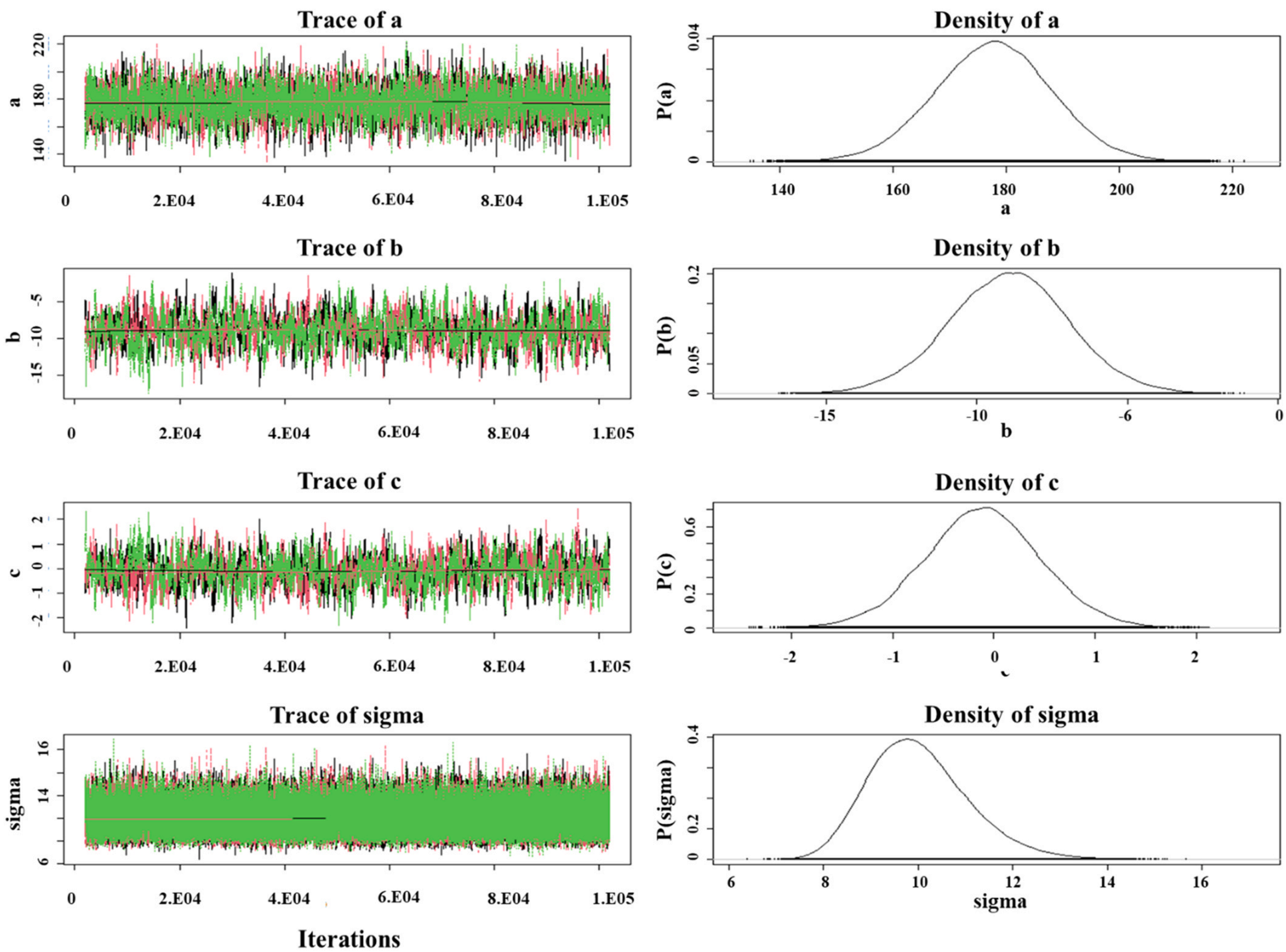

Fig. 2. Trace plots (on the left) and predicted posterior distributions (on the right) for the unknown parameters of the first model.

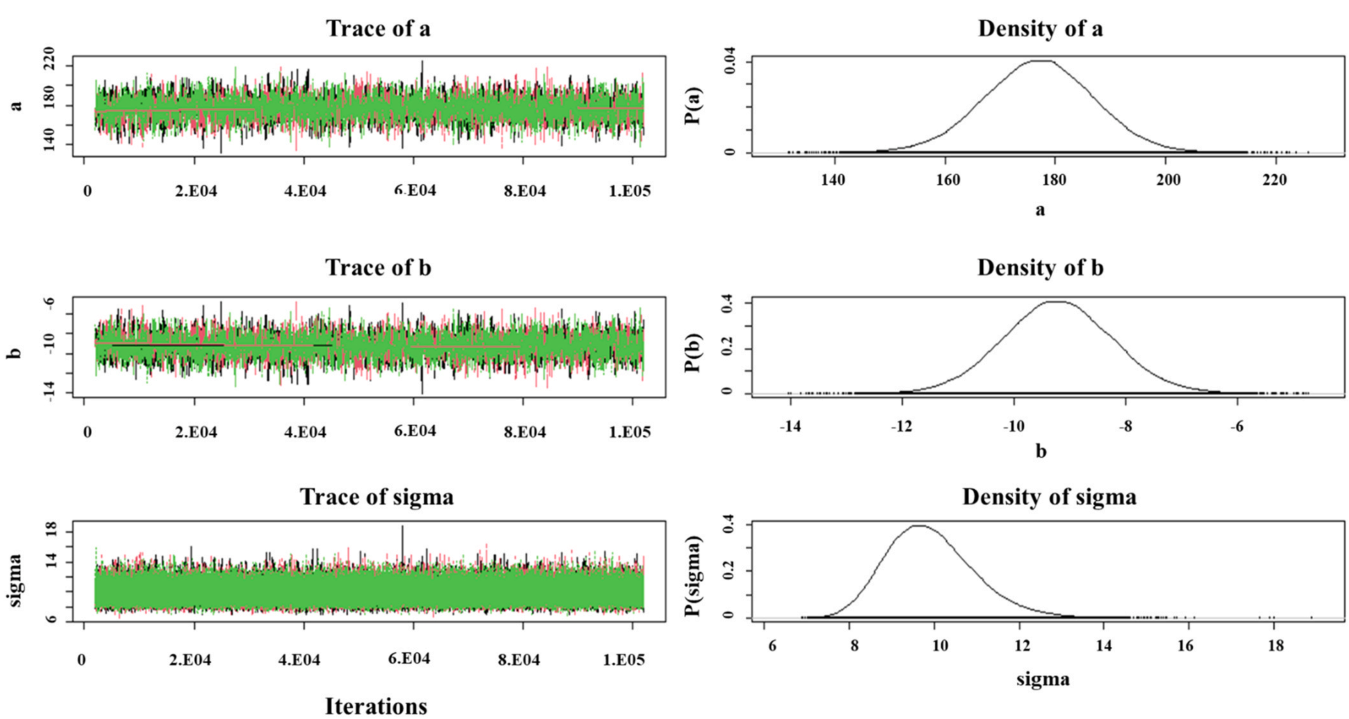

Fig. 3. Trace plots (on the left) and predicted posterior distributions (on the right) for the unknown parameters of the second model.

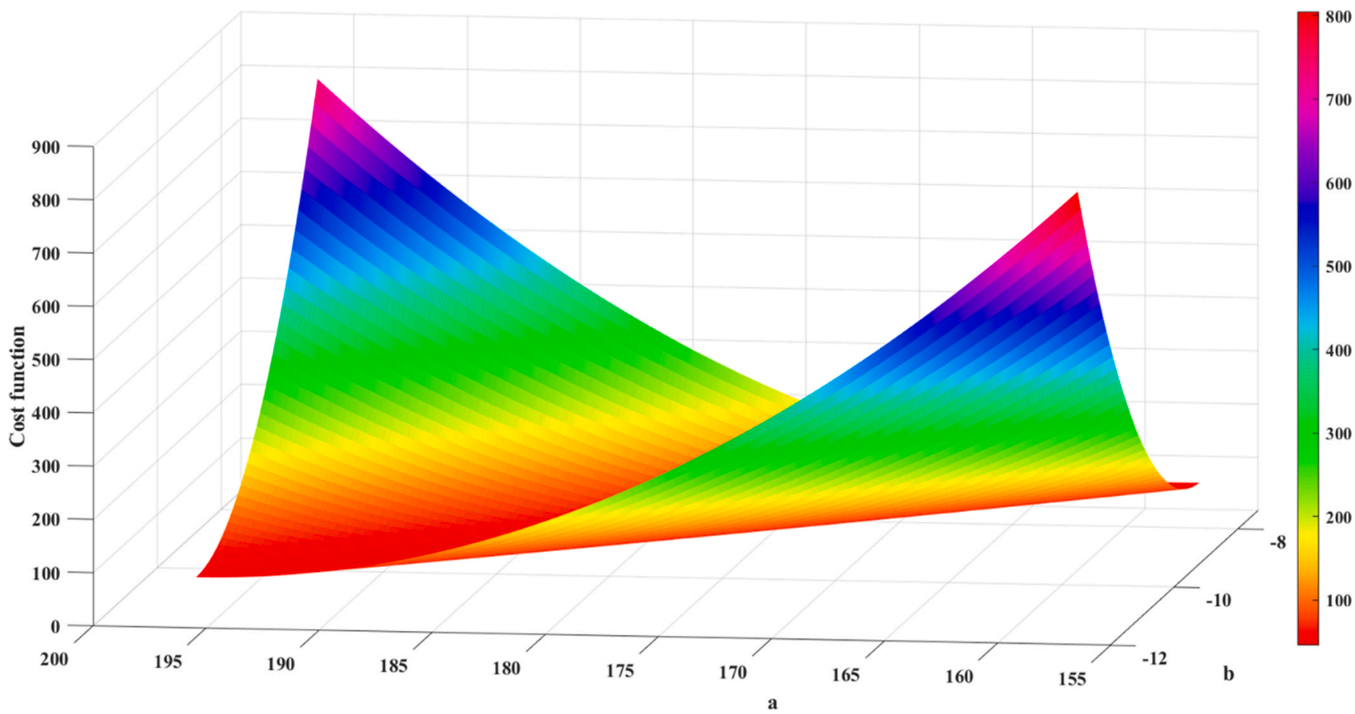

Fig. 4. 3D surface of the cost function.

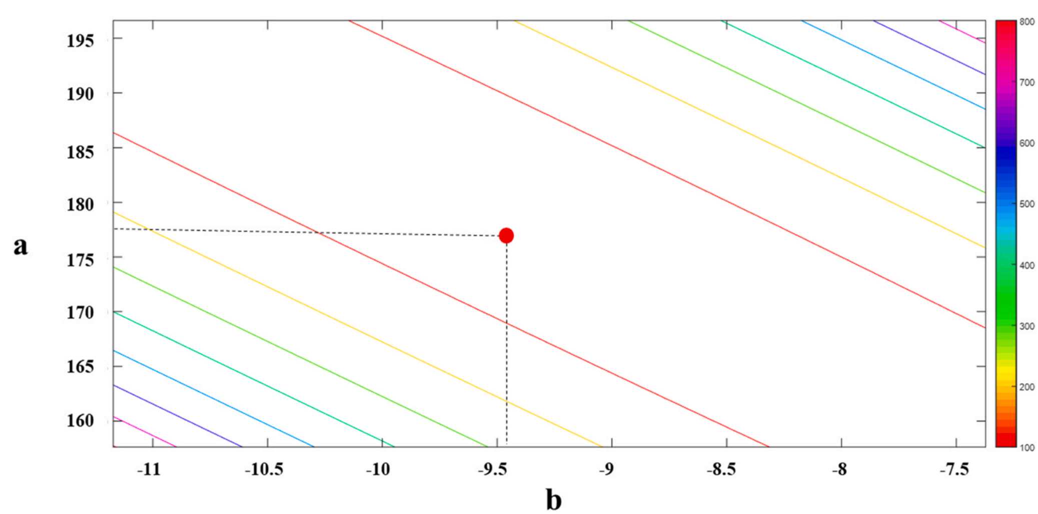

Fig. 5. Contour plot of the cost function. The red dot represents the minimum value.

function obtained is shown in Fig. 4, while the contour plot is illustrated in Fig. 5.

The minimum value of the cost function is equal to 45.6 and it is located at $(b, a) = (-9.472,179.52)$, which is pretty close to the mean value extracted through the HBR.

4.4. Stage 4: reliability estimation and maintenance scheduling

Given a working component in a standard operating environment, the reliability decreases over time because of a degradation process that is affected by the operating condition and the process variables. For this study, the reference threshold of the reliability is set equal to 0.4 (step 12), accordingly as soon as the estimated reliability reaches this value, the operations are not regarded as safe and an intervention is required. In other words, the threshold identifies the lowest acceptable value for the estimated reliability. The reliability threshold should be chosen based on company policies, expert judgments, guidelines, or regulations. considering the second regression model, the PV of interest is the pressure monitored during the operation (Step 13). Fig. 6 shows the pressure observed during 500 h of operation.

Next, the reliability is estimated considering a normal distribution, whose probability density function is given by Eq. (18).

$$f(t) = \frac{1}{\sigma\sqrt{2\pi}}e^{-\frac{1}{2}\left(\frac{t-\mu_t}{\sigma}\right)^2} \tag{18}$$

where μ_t is obtained by Eq. (12), considering the predicted parameters listed in Table 4 and the monitored pressure for t. Thus, each time unit is associated with a different value of μ_t based on the measured pressure. Since time is considered discrete, the unreliability is approximated, as shown by Eq. (19).

$$F(T) = \sum_{t=1}^{T}\frac{1}{\sigma\sqrt{2\pi}}e^{-\frac{1}{2}\left(\frac{t-\mu_t}{\sigma}\right)^2} \tag{19}$$

The reliability of each time unit is subsequently estimated as the complement to one of the unreliability, as depicted by Eq. (20).

$$R(T) = 1 - \sum_{t=1}^{T}\frac{1}{\sigma\sqrt{2\pi}}e^{-\frac{1}{2}\left(\frac{t-\mu_t}{\sigma}\right)^2} \tag{20}$$

Following Eq. (19), the reliability is estimated for each hour of the considered timespan (step 14). Given the reliability threshold mentioned above, a maintenance task is planned when the estimated reliability is less than 0.4 (step 15). Whenever a maintenance task is performed, the component is replaced with a new one, considering a replacement “as good as new” (AGAN). Consequently, the reliability is equal to 1 after the component is replaced. The estimated reliability and the scheduled maintenance tasks during the considered time interval are illustrated in Fig. 7. The calculation depicts three maintenance interventions: the first replacement is performed after 158 h of operation, while the second and third are carried out after 306 and 453 h, respectively. In Fig. 7, the red dotted lines represent a maintenance task (158, 306, and 453 h), while the gray horizontal dotted line represents the reliability threshold (0.4).

5. Discussion

5.1. Alternative model

The regression model with only the pressure as relevant PV is depicted as the best due to the lower DIC and the consistent Bayesian p-value. Moreover, the posterior mean value of the temperature coefficient related to the first model revealed less influence of the temperature on the reliability indicator. Since the pressure is regarded as the most influential PV, it is worth investigating another model characterized by a quadratic dependence of the MTTF regarding the pressure. The aforementioned model is illustrated by Eq. (21).

$$\mu = MTTF = a + b^{*}Press + c^{*}Press^2 \tag{21}$$

By adopting the same prior distributions introduced in Section 3.2 the statistical summary reported in Table 5 is got.

The calculation revealed a mean p-value of 0.4985, which is an acceptable value. However, looking at the trace plot shown in Fig. 8, the convergence is not reached. Consequently, the developed model could not be accepted as valid and must be discarded.

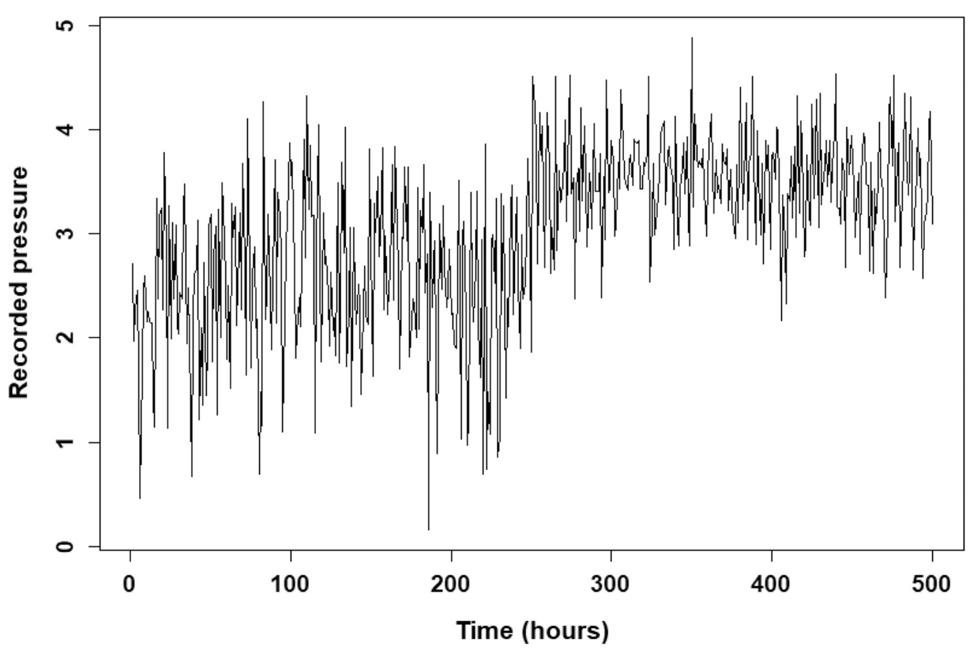

Fig. 6. Monitored pressure during 500 h of operation.

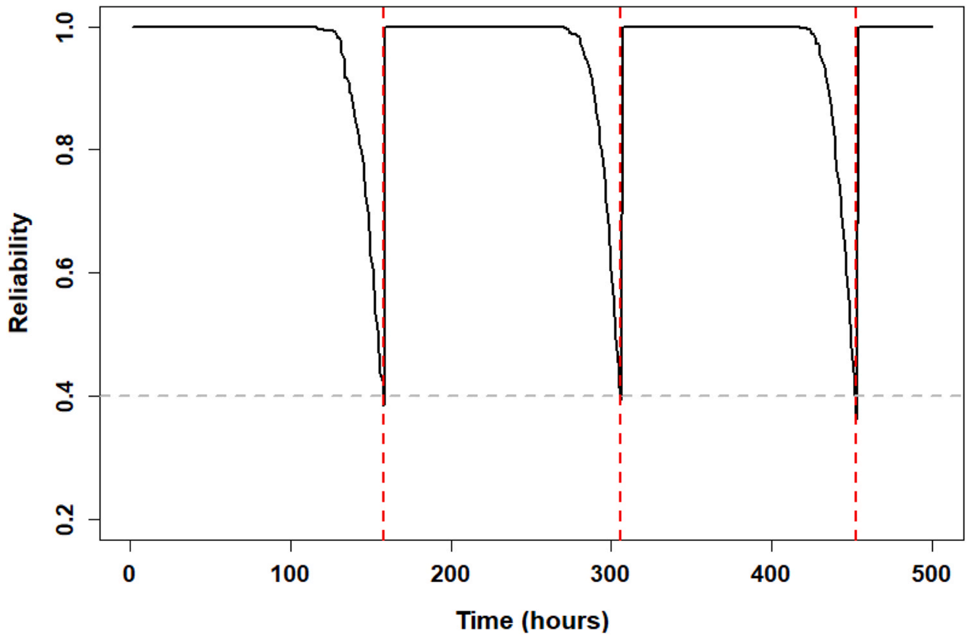

Fig. 7. Estimated reliability for each time unit based on the monitored pressure over a 500 h period.

5.2. Corrective maintenance and nonoperating time

Fig. 5 is got considering no failure between two preventive maintenance tasks. However, failures could occur even if a CBM policy is implemented. During the non-operating time, the unreliability is often considered constant; thus, it does not increase. Both CM and standby period could be easily added into the developed method. Indeed, whenever a failure occurs, a CM task is carried out, restoring the AGAN condition (the reliability is reset to 1). Subsequently, the monitoring process is reestablished until the occurrence of another failure or the preventive maintenance requirements are met. Regarding the nonoperating time, let t be the instant of shutdown and $t + n$ the time at which the operations are restarted. To model the absence of degradation, the condition defined by Eq. (22) is imposed.

$$F(t) = F(t + n) \tag{22}$$

where $F(t)$ is the estimated unreliability in t, while $F(t + n)$ is the assigned unreliability for $t + n$. Through Eq. (21), the unreliability is maintained constant, which is equal to constant reliability during the non-operating period. As an example, a component operating under a normal TTF distribution whose parameters are listed in Table 4 is considered. The history of the component state is shown in Fig. 9, along with the recorded pressure. Table 6 reports a summary of the relevant events along with their occurrence time. Before reliability drops below the threshold, a failure is observed after 130 h of operation and a CM task is performed. Subsequently, the device

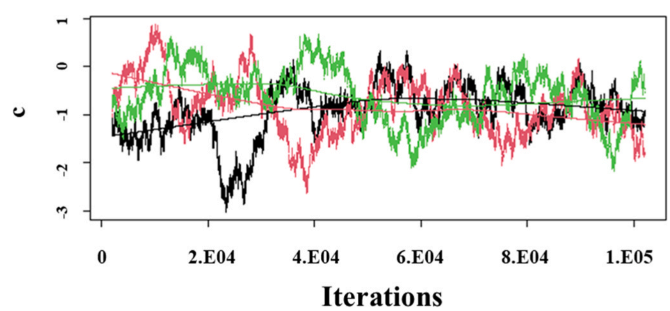

Fig. 8. Trace plot of c (quadratic pressure coefficient), illustrating the absence of convergence for the developed regression model.

operates until the estimated reliability reaches the threshold value of 0.4, leading to a PM intervention after 279 h of operations. Next, another PM action is performed after 422 h of operation. Finally, 552 h after the start of the operation, the pressure drops to 0, identifying a standby state. Accordingly, the reliability of the component is kept equal to the reliability estimated during the last operating hour until a new operating state is observed. Considering Fig. 9, a) reports the pressure and the reliability till the CM is performed, while b) and c) displays the monitored pressure and the estimated reliability till the first and the second PM task, respectively. Finally, d) illustrates the pressure and the reliability until the end of the considered period.

Table 5
Statistical summary of the posterior parameters associated with the model with quadratic pressure dependence.

Parameter	Mean	Standard deviation	2.5 percentile	97.5 percentile
a	100.251	57.6577	-24.168	208.8459
b	6.5604	11.7032	-15.343	31.6898
c	-0.795	0.5866	-2.062	0.3025
sigma	10.0788	1.068	8.25	12.4237

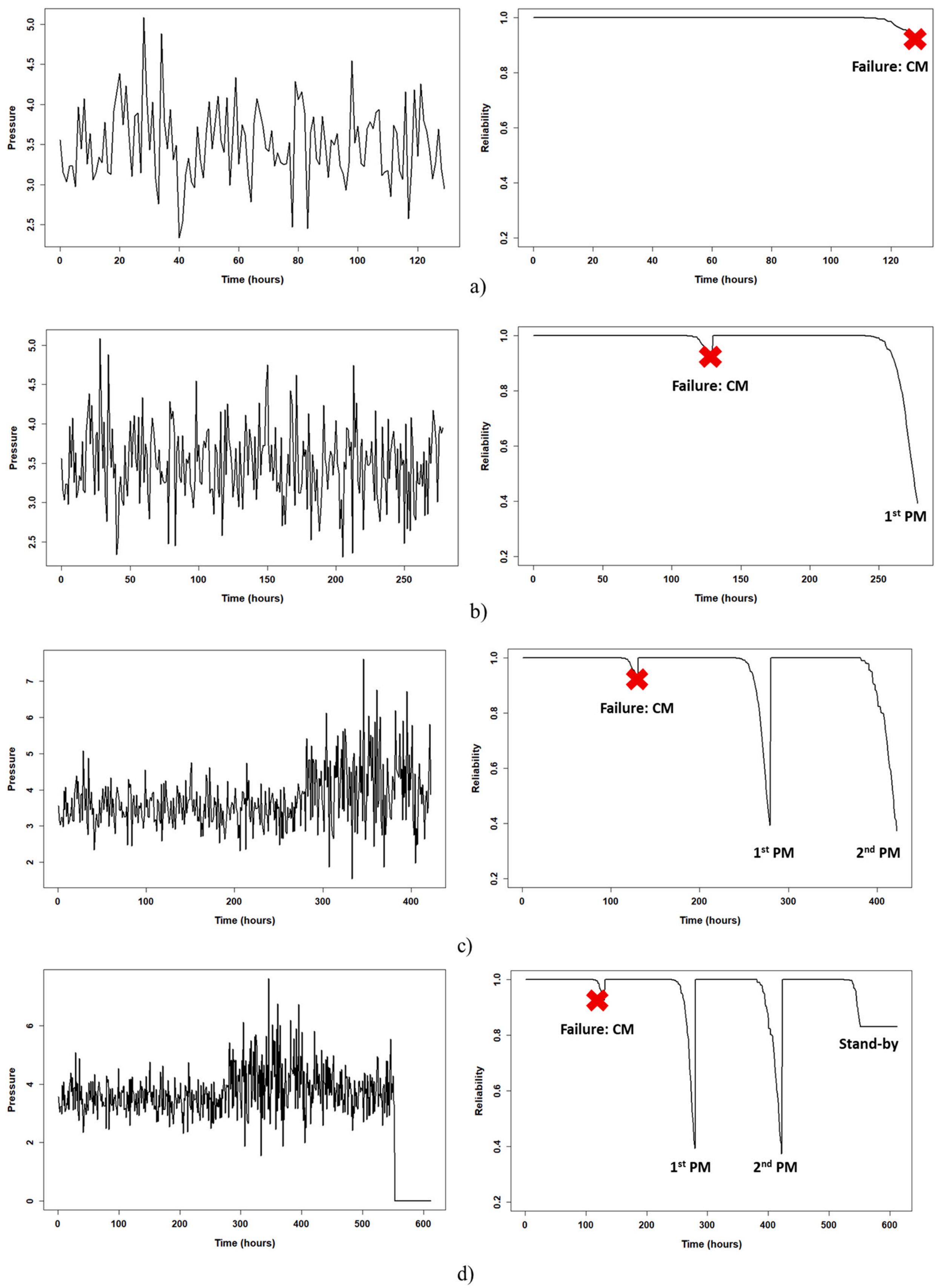

Fig. 9. Integration of CM and non-operating time to the developed methodology for the presented example.

Table 6
List of the sequence of relevant events. PM denotes a PM task, while CM represents a CM task. Finally, SB identifies a transition to a standby state.

Time	130	279	422	552
Relevant event	CM	PM	PM	SB

6. Conclusions and future studies

This paper presents a novel methodology capable of developing a regression model between PVs and RIs through the exploitation of data extracted from ALT. The obtained regression function is then used for conducting an online reliability estimation. In the framework developed, HBR and GLM were integrated to determine the link function between the covariates and the dependent variable (that is, RI). A normal-normal regression model was chosen, considering the MTTF as RI, while pressure and temperature were chosen as relevant PVs. The HBR was implemented on data extracted from five distinct operating conditions, while two distinct regression models were considered. Showing a lower DIC, the model with only the pressure is selected as the best. Subsequently, the Bayesian inference is used for the online reliability estimation, considering the pressure values detected during 500 working hours. Setting a reliability threshold equal to 0.4, three maintenance tasks after 158, 306, and 453 h respectively emerged from the calculation. Finally, an extension with corrective maintenance and nonoperating time is presented.

The presented approach could be adopted in any operational context where a manufacturer is testing its products through ALT. Indeed, a controlled operating environment is required to determine the relationship between the most relevant PVs and RI at first, and subsequently estimate the reliability during use. Consequently, the method could be useful both for the design and for the operating phases. During the design phase, the framework could assist the enterprises to test whether the reliability requirements are satisfied, while during the operating phase it could be helpful to optimize postsale services.

Among the limitations of the developed framework, it is worthwhile to mention the absence of imperfect maintenance tasks and measurement errors arising from sensors. Thus, including these two aspects in future developments could be relevant to make the methods more realistic. Indeed, any kind of maintenance task could be affected by process error, leading to partially restoring the life of the maintained device. Additionally, measurement errors could influence the decision process related to maintenance planning. Another important limitation of the present work is that maintenance actions are considered instantaneous (i.e., with no delay between the trigger and the start of the maintenance action). Future work could consider a maintenance delay related to logistics and resource issues, anticipating the maintenance trigger based on the delay distribution and predictions regarding the values assumed by the PVs. Addressing these considerations will result in a prognostic approach. Furthermore, considering a real application could require some amendments to the framework, thus the authors are planning to test the developed framework on real industrial data. Finally, the comparison between this framework and other classic approaches could be useful to determine the advantages and disadvantages of each method, thus the authors are planning to work on this topic as well.

Declaration of Competing Interest

The authors declare that they have no known competing financial interests or personal relationships that could have appeared to influence the work reported in this paper.

References

BahooToroody, A., Abaei, M.M., Arzaghi, E., BahooToroody, F., De Carlo, F., Abbassi, R., 2019a. Multi-level optimization of maintenance plan for natural gas system exposed to deterioration process. J. Hazard. Mater. 362, 412–423.
BahooToroody, A., Abaei, M.M., Arzaghi, E., Song, G., De Carlo, F., Paltrinieri, N., Abbassi, R., 2020a. On reliability challenges of repairable systems using hierarchical bayesian inference and maximum likelihood estimation. Process Saf. Environ. Prot. 135, 157–165.
BahooToroody, A., Abaei, M.M., BahooToroody, F., De Carlo, F., Abbassi, R., Khalaj, S., 2019b. A condition monitoring based signal filtering approach for dynamic time dependent safety assessment of natural gas distribution process. Process Saf. Environ. Prot. 123, 335–343.
BahooToroody, A., De Carlo, F., Paltrinieri, N., Tucci, M., Van Gelder, P., 2020b. Bayesian regression based condition monitoring approach for effective reliability prediction of random processes in autonomous energy supply operation. Reliab. Eng. Syst. Saf. 201, 106966.
Baptista, M., Sankararaman, S., de Medeiros, I.P., Nascimento Jr., C., Prendinger, H., Henriques, E.M., 2018. Forecasting fault events for predictive maintenance using data-driven techniques and ARMA modeling. Comput. Ind. Eng. 115, 41–53.
Benkedjouh, T., Zerhouni, N., Rechak, S., 2018. Tool wear condition monitoring based on continuous wavelet transform and blind source separation. Int. J. Adv. Manuf. Technol. 97 (9), 3311–3323.
Brito, L.C., Susto, G.A., Brito, J.N., Duarte, M.A., 2022. An explainable artificial intelligence approach for unsupervised fault detection and diagnosis in rotating machinery. Mech. Syst. Signal Process. 163, 108105.
Cipollini, F., Oneto, L., Coraddu, A., Murphy, A.J., Anguita, D., 2018. Condition-based maintenance of naval propulsion systems with supervised data analysis. Ocean Eng. 149, 268–278.
Dave, H.B., Singh, D., Bansal, H.O., 2021. Multiple linear regression-based impact analysis of impedance network design on life expectancy of DC-link capacitor in q-ZSI fed motor drive. Eng. Sci. Technol., Int. J. 24 (1), 171–182.
El-Gheriani, M., Khan, F., Chen, D., Abbassi, R., 2017. Major accident modelling using spare data. Process Saf. Environ. Prot. 106, 52–59.
Elsayed, E.A., 2012. Overview of reliability testing. IEEE Trans. Reliab. 61 (2), 282–291.
Escobar, L.A., Meeker, W.Q., 2006. A review of accelerated test models. Stat. Sci. 552–577.
Ferrando Chacón, J.L., Fernández de Barrena, T., García, A., Sáez de Buruaga, M., Badiola, X., Vicente, J., 2021. A novel machine learning-based methodology for tool wear prediction using acoustic emission signals. Sensors 21 (17), 5984.
Follmann, D., Wu, M., 1995. An approximate generalized linear model with random effects for informative missing data. Biometrics 151–168.
Garthwaite, P.H., Jolliffe, I.T., Jolliffe, I., & Jones, B., 2002, Statistical inference: Oxford University Press on Demand.
Gowid, S., Dixon, R., Ghani, S., 2015. A novel robust automated FFT-based segmentation and features selection algorithm for acoustic emission condition based monitoring systems. Appl. Acoust. 88, 66–74.
Guisan, A., Edwards Jr., T.C., Hastie, T., 2002. Generalized linear and generalized additive models in studies of species distributions: setting the scene. Ecol. Model. 157 (2–3), 89–100.
Haghighi, F., 2014. Optimal design of accelerated life tests for an extension of the exponential distribution. Reliab. Eng. Syst. Saf. 131, 251–256.
Hamada, M.S., Martz, H.F., Reese, C.S., Wilson, A.G., 2008. Bayesian Reliability Vol. 15 Springer.
Hao, S., Yang, J., Berenguer, C., 2020. Condition-based maintenance with imperfect inspections for continuous degradation processes. Appl. Math. Model. 86, 311–334.
Hu, J., Xu, A., Li, B., Liao, H., 2021. Condition-based maintenance planning for multi-state systems under time-varying environmental conditions. Comput. Ind. Eng. 158, 107380.
Jardine, A.K., Lin, D., Banjevic, D., 2006. A review on machinery diagnostics and prognostics implementing condition-based maintenance. Mech. Syst. Signal Process. 20 (7), 1483–1510.
Jiang, A., Huang, Z., Xu, J., Xu, X., 2021. Condition-based opportunistic maintenance policy for a series–parallel hybrid system with economic dependence. J. Qual. Maint. Eng.
Kelly, D., Smith, C., 2011. Bayesian Inference for Probabilistic Risk Assessment: A Practitioner's Guidebook. Springer Science & Business Media.
Kelly, D.L., Smith, C.L., 2009. Bayesian inference in probabilistic risk assessment—the current state of the art. Reliab. Eng. Syst. Saf. 94 (2), 628–643.
Kumari, P., Lee, D., Wang, Q., Karim, M.N., Sang-Il Kwon, J., 2020. Root cause analysis of key process variable deviation for rare events in the chemical process industry. Ind. Eng. Chem. Res. 59 (23), 10987–10999.
Leoni, L., BahooToroody, F., Khalaj, S., Carlo, F.D., BahooToroody, A., Abaei, M.M., 2021. Bayesian estimation for reliability engineering: Addressing the influence of prior choice. Int. J. Environ. Res. Public Health 18 (7), 3349.
Lin, K., Chen, Y., Xu, D., 2017. Reliability assessment model considering heterogeneous population in a multiple stresses accelerated test. Reliab. Eng. Syst. Saf. 165, 134–143.
Liu, X., 2012. Planning of accelerated life tests with dependent failure modes based on a gamma frailty model. Technometrics 54 (4), 398–409.
Memala, W.A. , Bhuvaneswari, C. , Mana, S.C. , Selvan, M.P. , Maniraj, M. , & Kishore, S., 2021, An Approach to Remote Condition monitoring of Electrical Machines based on IOT. Paper presented at the Journal of Physics: Conference Series.

Morimoto, A., Sato, Y., Takata, S., 2017. Continuous improvement of criteria for condition-based maintenance by means of effects evaluation of treatments. Procedia CIRP 61, 293–298.
Moustafa, K., Hu, Z., Mourelatos, Z.P., Baseski, I., Majcher, M., 2021. System reliability analysis using component-level and system-level accelerated life testing. Reliab. Eng. Syst. Saf. 214, 107755.
Murphy, K.P., 2012. Machine Learning: A Probabilistic Perspective. MIT Press.
Omshi, E.M., Grall, A., 2021. Replacement and imperfect repair of deteriorating system: Study of a CBM policy and impact of repair efficiency. Reliab. Eng. Syst. Saf. 215, 107905.
Pandarakone, S.E., Akahori, K., Matsumura, T., Mizuno, Y., & Nakamura, H. (2017). *Development of a methodology for bearing fault scrutiny and diagnosis using SVM*. Paper presented at the 2017 IEEE International Conference on Industrial Technology (ICIT).
Pang, Z., Si, X., Hu, C., Du, D., Pei, H., 2021. A Bayesian Inference for Remaining Useful Life Estimation by Fusing Accelerated Degradation Data and Condition Monitoring Data. Reliab. Eng. Syst. Saf. 208, 107341.
Pascual, F. , Meeker, W.Q. , & Escobar, L.A., 2006, Accelerated life test models and data analysis. Handbook of Engineering Statistics (H. Pham, ed.) Chapter, 22.
Potočnik, P., Govekar, E., 2017. Semi-supervised vibration-based classification and condition monitoring of compressors. Mech. Syst. Signal Process. 93, 51–65.
Prajapati, A., Bechtel, J., Ganesan, S., 2012. Condition based maintenance: a survey. J. Qual. Maint. Eng.
Roy, S., 2018. Bayesian accelerated life test plans for series systems with Weibull component lifetimes. Appl. Math. Model. 62, 383–403.
Thomas, E.V., 2015, A Statistical Perspective on Highly Accelerated Testing. Retrieved from.
Tucci, M., De Carlo, F., Borgia, O., Fanciullacci, N., 2014. Accelerated life tests as an integrated methodology for product design, qualification and production control: a case study in household appliances. Prod. Manuf. Res. 2 (1), 112–127.
van den Hoogen, J., Bloemheuvel, S., Atzmueller, M., 2021. Classifying multivariate signals in rolling bearing fault detection using adaptive Wide-Kernel CNNs. Appl. Sci. 11 (23), 11429.
Wang, X., Sun, P., Sun, L., Luo, Q., Du, X., 2020. Online Condition Monitoring for Bond Wire Degradation of IGBT Modules in Three-Level Neutral-Point-Clamped Converters. IEEE Trans. Ind. Electron.
Xu, J., Liang, Z., Li, Y.-F., Wang, K., 2021. Generalized condition-based maintenance optimization for multi-component systems considering stochastic dependency and imperfect maintenance. Reliab. Eng. Syst. Saf. 211, 107592.
Ye, Z.-S., Hong, Y., Xie, Y., 2013. How do heterogeneities in operating environments affect field failure predictions and test planning? Ann. Appl. Stat. 2249–2271.
Ye, Z.S., Xie, M., 2015. Stochastic modelling and analysis of degradation for highly reliable products. Appl. Stoch. Models Bus. Ind. 31 (1), 16–32.
Yeganeh, A., Shadman, A., 2021. Using evolutionary artificial neural networks in monitoring binary and polytomous logistic profiles. J. Manuf. Syst. 61, 546–561.
Zeger, S.L., Karim, M.R., 1991. Generalized linear models with random effects; a Gibbs sampling approach. J. Am. Stat. Assoc. 86 (413), 79–86.
Zhang, J., Du, X., Qian, C., Tai, H.-M., 2021. A quasi-online condition monitoring technique for the wind power converter. Int. J. Electr. Power Energy Syst. 130, 106971.